Simulation Study on the Concept of Lifetime-Equivalent Defect Density in the Context of Light-Induced Degradation (LID) Experiments

Axel Herguth

University of Konstanz, 78464 Konstanz

***Abstract* — The concept of lifetime-equivalent defect density in the context of light-induced degradation investigation is evaluated by means of simulations especially in cases where more than one defect species changes over time. The superposition of boron-oxygen related light-induced degradation (BO-LID) with light- and elevated temperature-induced degradation (LeTID) as well as FeB dissociation as found in reality is discussed. Furthermore, the effect of varying background lifetime, as often encountered in the context of LeTID in mc-Si, and varying Fe density is studied.**

***Index Terms* — defect kinetics, LID, BO-LID, LeTID, FeB**

I. Introduction

In many studies on defect formation and especially in the context of light-induced degradation (LID), *e.g.* [1]-[12], defect dynamics are studied using the synonymous quantity "effective, normalized, relative or lifetime-equivalent defect density ΔN_{leq}"

$$\Delta N_{\mathrm{leq}} := \frac{1}{\tau_{\mathrm{eff}}(t)} - \frac{1}{\tau_{\mathrm{eff}}(t_0)} = \frac{1}{f} \cdot \Delta N_{\mathrm{SRH}} \qquad (1)$$

where $\tau_{\mathrm{eff}}(t)$ is the effective excess charge carrier lifetime changing over time t and $\tau_{\mathrm{eff}}(t_0)$ is used as a reference at a certain point in time t_0. This lifetime-equivalent defect density ΔN_{leq}, given in units of [s^{-1}] and not as the term "density" might imply in units of [cm^{-3}], has proven to be a valuable quantity because it is directly proportional to the change in actual defect density N_{SRH} of a single bulk defect species with its lifetime given, *e.g.*, by Shockley-Read and Hall's (SRH) theory [13], [14] as

$$\frac{1}{\tau_{\mathrm{SRH}}} = \frac{(n_0+p_0+\Delta n)}{\frac{n_0+\Delta n+n_1}{\sigma_{\mathrm{p}}\nu_{\mathrm{th,p}}}+\frac{p_0+\Delta n+p_1}{\sigma_{\mathrm{n}}\nu_{\mathrm{th,n}}}} \cdot N_{\mathrm{SRH}} = \frac{1}{f} \cdot N_{\mathrm{SRH}} \qquad (2)$$

because taking the difference of inverse effective lifetimes comprising multiple recombination channels

$$\frac{1}{\tau_{\mathrm{eff}}} = \frac{1}{\tau_{\mathrm{int}}} + \frac{1}{\tau_{\mathrm{surface}}} + \sum_j \frac{1}{\tau_{\mathrm{SRH},j}} \qquad (3)$$

cancels out any lifetime component not variable in time, be it surface, intrinsic or bulk (SRH) defect related. A more detailed derivation of ΔN_{leq} and its properties can be found in [15].

However, it should be noted that (i) ΔN_{leq} (like τ_{SRH}) depends specifically on injection Δn via the pre-factor $f(\Delta n)$ defined in Eq. 2, (ii) ΔN_{leq} only depicts the change in N_{SRH} occurring from t_0 to t and not absolute N_{SRH}, and (iii) Eq. 1 describes the change of only one defect. If a multitude of j different defects changes in parallel, Eq. 1 expands to

$$\Delta N_{\mathrm{leq}} = \sum_j \frac{1}{f_j} \cdot \Delta N_j = \sum_j \Delta N_{\mathrm{leq},j} \qquad (4)$$

and ΔN_{leq} corresponds to an f_j-weighed sum of individually changing defect densities ΔN_j.

In the following, different scenarios are studied by means of simulations demonstrating that ΔN_{leq} can offer insights in defect dynamics but is also prone to misinterpretation.

II. Simulation Details

Three different defect types shall be discussed in the following: (i) a deep defect with τ_n = 50 µs and τ_p/τ_n = 10 which resembles the defect species responsible for boron-oxygen related light-induced degradation (BO-LID) [2], [6]; (ii) a deep defect with τ_n = 35 µs and τ_p/τ_n = 30 which resembles the defect species responsible for light- and elevated temperature-induced degradation (LeTID) [9], [16]-[19]; and (iii) iron at a density of $5\cdot10^{10}$ cm^{-3} which prefers either to form FeB pairs with boron at room temperature in darkness, or to sit in an interstitial site at elevated temperatures and/or excess charge carrier injection [20]-[23]. The association or dissociation of these FeB pairs is assumed to occur completely. Apart from these defect types, effective lifetime τ_{eff} is considered to be only limited by intrinsic or surface-related recombination. The latter one is parametrized in terms of a J_0 model with J_0 = 15 fA/cm^2 (per side) [24]. However, as both are assumed constant, they cancel out anyway when ΔN_{leq} is calculated. Figures 1 and 2 depict the lifetime components of those defects in p-type material (doping $p_0 = 1\cdot10^{16}$ cm^{-3}) and the resulting effective lifetime in the injection range typically used in lifetime studies using the photoconductance decay method.

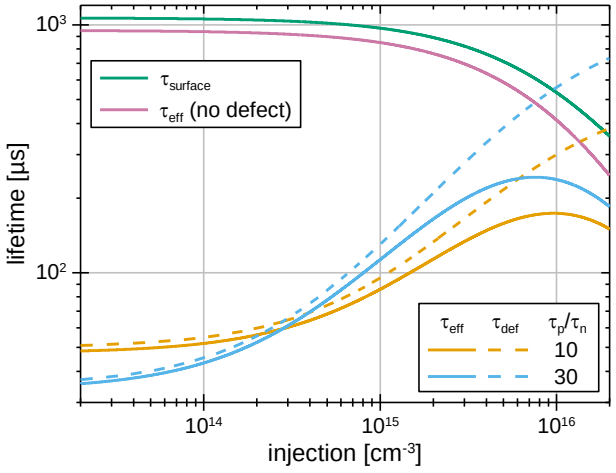

Fig. 1. Injection-dependent lifetime components τ_{def} of the first two defect species as well as effective lifetime τ_{eff} resulting from the superposition of the respective defect species with intrinsic and surface recombination. (T = 300 K, $p_0 = 1\cdot10^{16}$ cm^{-3})

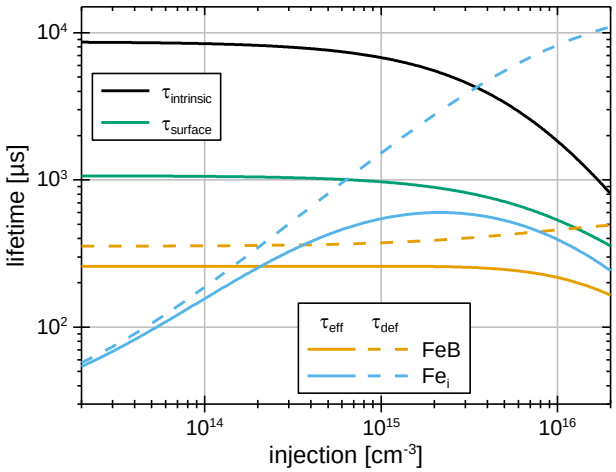

Fig. 2. Injection-dependent lifetime components τ_{def} of FeB and Fe_i as well as effective lifetime τ_{eff} resulting from the superposition with intrinsic and surface recombination. (T = 300 K, $p_0 = 1{\cdot}10^{16}\,cm^{-3}$)

The strong difference in carrier capture cross-sections of FeB ($\sigma_p = 5{\cdot}10^{-15}\,cm^2$, $\sigma_n = 3{\cdot}10^{-15}\,cm^2$) and Fe_i ($\sigma_p = 7{\cdot}10^{-17}\,cm^2$, $\sigma_n = 4{\cdot}10^{-14}\,cm^2$) results in a characteristic cross-over point (cop) of the lifetime curves at $\Delta n_{cop} \sim 2{\cdot}10^{14}\,cm^{-3}$ [20]-[23]. This characteristic behavior of iron allows for a comparatively easy quantification of iron in silicon by intentionally switching iron between those states by illumination (FeB dissociation) and dark storage at room temperature (FeB association). However, unintentional dissociation after dark storage is a nuisance during light-induced degradation studies.

Figure 3 shows the lifetime-equivalent defect density ΔN_{leq} determined from the lifetime data in Fig. 1 using the defect-free effective lifetime $\tau_{eff,nodef}$ as reference and from $\tau_{eff,Fe}$ in Fig. 2 using the associated state (FeB) as reference. It should be noted that the τ_p/τ_n ratio translates directly from τ_{SRH} to ΔN_{leq} and thus ΔN_{leq} strongly increases for decreasing injection for deep defects. It is therefore important to state always the injection at which ΔN_{leq} was determined together with substrate doping p_0 because τ_{SRH} (Eq. 2) shifts with injection relative to p_0.

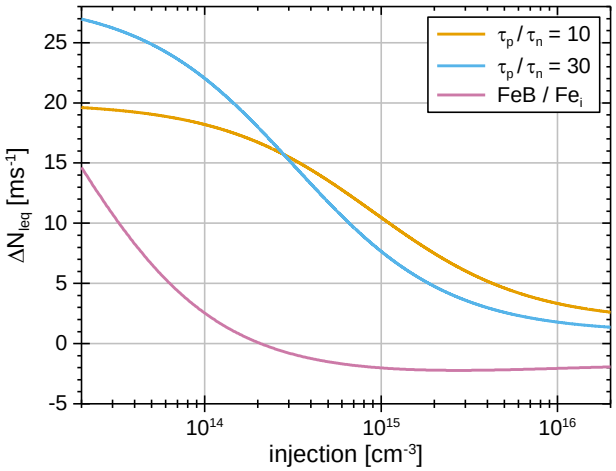

Fig. 3. Injection-dependent lifetime-equivalent defect density ΔN_{leq} determined from Figs. 1 and 2. (T = 300 K, $p_0 = 1{\cdot}10^{16}\,cm^{-3}$)

Describing the dissociation of FeB to Fe_i in terms of ΔN_{leq} yields at first glance a counter-intuitive behavior of ΔN_{leq}. While ΔN_{leq} is positive below the cross-over point and one would conclude that defects have formed, it becomes negative above the cross-over point and one would conclude that defects have vanished even though total iron concentration has of course not changed. Whether the FeB pairs completely dissociate or not, is irrelevant here because the influence of still associated FeB pairs cancels out when ΔN_{leq} is calculated.

III. Simulated Defect Dynamics

Three different scenarios are presented in the following. In a first *scenario A*, that shall resemble BO-LID, a single defect species forms and vanishes over the course of time. In a second *scenario B*, a second defect species, that shall resemble LeTID, forms and vanishes in parallel to the first defect species (extending *scenario A*). In a third *scenario C*, the dynamic of these two defect species is superimposed with the dissociation of FeB (extending *scenario B*). The increase and subsequent decrease of respective defect densities N_x in *scenarios A & B* related to the two defect species, resulting in a degradation and regeneration of lifetime, is assumed to follow the equation [25]

$$N_x(t) = -N_{1,x} \cdot \exp\left(-\frac{t}{t_{deg,x}}\right) + N_{2,x} \cdot \exp\left(-\frac{t}{t_{reg,x}}\right) \quad (5)$$

with t_{deg} and t_{reg} being characteristic time constants of the respective degradation and regeneration phase. For the FeB dissociation, a simple exponential decay

$$\frac{[Fe_i]}{[Fe]_{total}} = 1 - \frac{[FeB]}{[Fe]_{total}} = 1 - \exp\left(-\frac{t}{t_{Fe}}\right) \quad (6)$$

with time constant t_{Fe} is assumed. As it is not the intention of this paper to depict a specific situation but rather to describe the general behavior, time t is treated as a dimensionless quantity. Thus only relative but not absolute time constants are relevant.

A. Scenario A: BO-LID

Boron-doped, oxygen-rich silicon (*e.g.* Cz-Si) is prone to the formation of a recombination-active defect species under excess charge carrier injection (*e.g.* by illumination) at low temperatures (< 100°C) resulting in a degradation of lifetime [2], [6]. However, it is also observed that illuminated annealing at elevated temperatures (> 50°C) can lead to a subsequent deactivation of the harmful defect species resulting in a slow regeneration of lifetime [25], [26]. Within this scenario, the fast degradation and slow regeneration are accounted for by using $t_{deg,BOLID}$ = 2.5 and $t_{reg,BOLID}$ = 25. Under the correct conditions, lifetime recovery can be almost complete [25] and therefore it is assumed here that $N_{1,BOLID} = N_{2,BOLID}$. Furthermore, it is assumed that the low injection lifetime of BO-LID drops to τ_n = 50 µs at maximum defect density (maximum of Eq. 5) and injection dependence is well described by $\tau_p/\tau_n = 10$ [2], [6]. This scenario could, *e.g.*, occur during illuminated annealing at a temperature of 75°C and 1 sun illumination intensity [27].

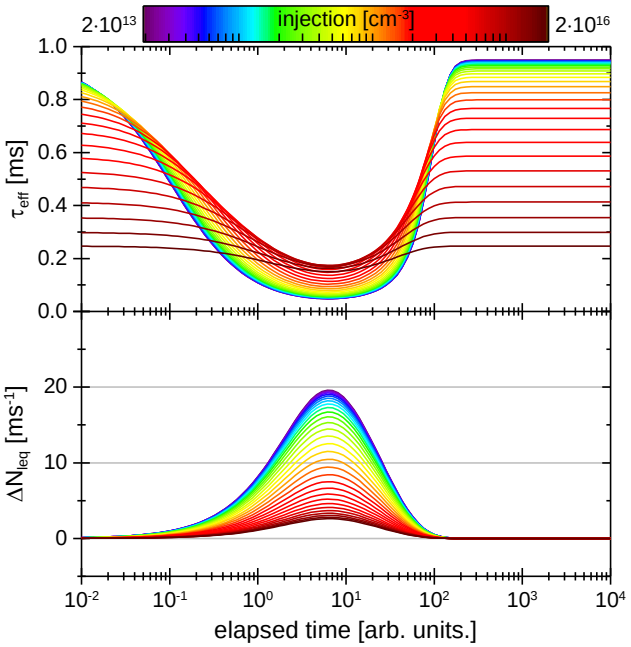

Fig. 4. Time-resolved evolution of the effective lifetime τ_{eff} and derived lifetime-equivalent defect density ΔN_{leq} at various color-coded injection levels Δn in *scenario A*. (T = 300 K, $p_0 = 1{\cdot}10^{16}$ cm^{-3})

The simulation results of *scenario A* are shown in Fig. 4. In the short and long term, when BO-LID degradation has not yet kicked-in or regeneration is already almost complete, τ_{eff} is limited by surface-related recombination (see Fig. 1) and thus τ_{eff} is almost injection-independent at low injection levels (violet to green colors) and decreases for high injection levels (yellow to red colors). In the medium term, BO-LID results in the expected inversion of the color order (being characteristic for a deep SRH defect) and the typical bathtub-like broad lifetime minimum at low injection becoming narrower at higher injection levels. Only after calculation of ΔN_{leq} it becomes obvious that the various (injection) color-coded lines depict the same defect dynamic and yield the same time constants even though the amplitude differs (see Fig. 3).

B. Scenario B: BO-LID and LeTID in parallel

Besides BO-LID, light- and elevated temperature-induced degradation (LeTID) [7]-[11], [16]-[19] seems to occur in Cz-Si as well [8], [12]. Like BO-LID, LeTID features not only a degradation but also a regeneration phase. Whether describing LeTID by Eq. 5 is perfectly correct or not is irrelevant here as the exact progression with time does not matter. At least at low temperatures (*e.g.* 75°C), both degradation and regeneration of lifetime due to LeTID occur on a longer time scale compared to BO-LID, however, some overlap occurs. Therefore, time constants of LeTID in *scenario B* are chosen to $t_{deg,LeTID} = 25$ and $t_{reg,LeTID} = 250$. Under the correct conditions, lifetime recovery seems to be almost complete and therefore it is assumed here that $N_{1,LeTID} = N_{2,LeTID}$. However, one should note that this might be a critical assumption in reality. Furthermore,

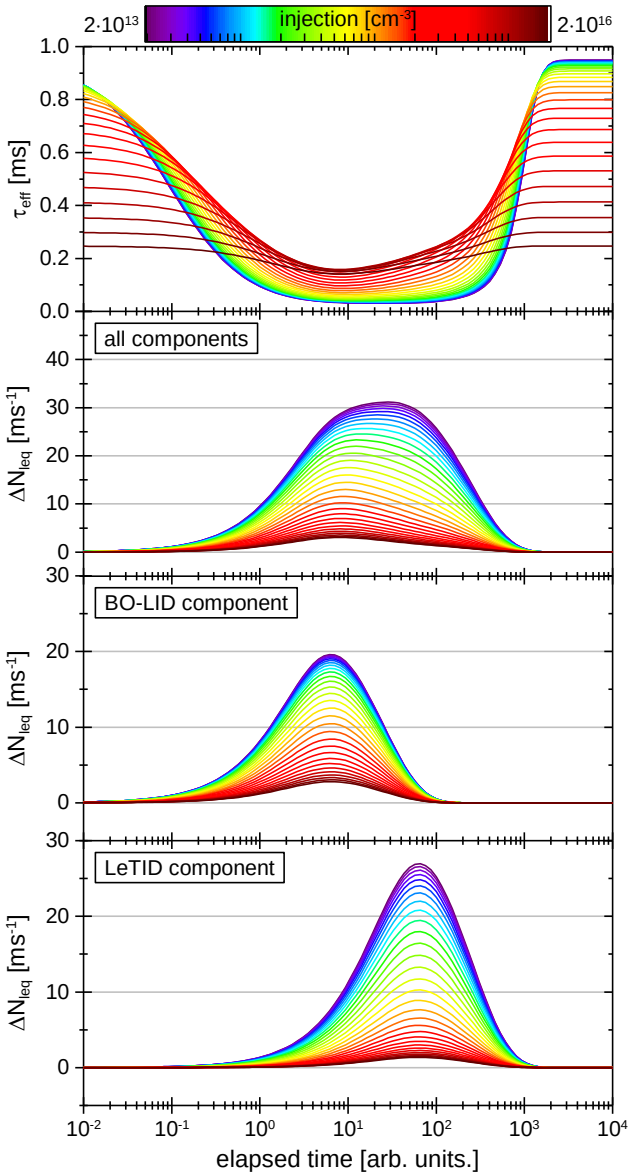

Fig. 5. Time-resolved evolution of the effective lifetime τ_{eff} and derived lifetime-equivalent defect density ΔN_{leq} (in total and for BO-LID and LeTID seperately) at various color-coded injection levels Δn in *scenario B*. (T = 300 K, $p_0 = 1{\cdot}10^{16}$ cm^{-3})

it is assumed that the low injection lifetime of LeTID drops to τ_n = 35 µs at maximum defect density and injection dependence is well described by $\tau_p/\tau_n = 30$ [19]. This *scenario B* could just like *scenario A*, *e.g.*, occur during illuminated annealing at a temperature of 75°C and 1 sun illumination intensity [27].

Figure 5 shows the simulation results of *scenario B*. The first thing to note is the broadening of the bathtub-like minimum in effective lifetime which, of course, results from the slower onset and subsequent recovery from LeTID. At first glance, especially if τ_{eff} and/or ΔN_{leq} are evaluated at an injection level of $\Delta n \sim 1{\cdot}10^{15}$ cm^{-3} (orange), there is no clear second minimum visible and one might conclude that the slow recovery is, for whatever reason, simply due to a slow regeneration of BO-LID.

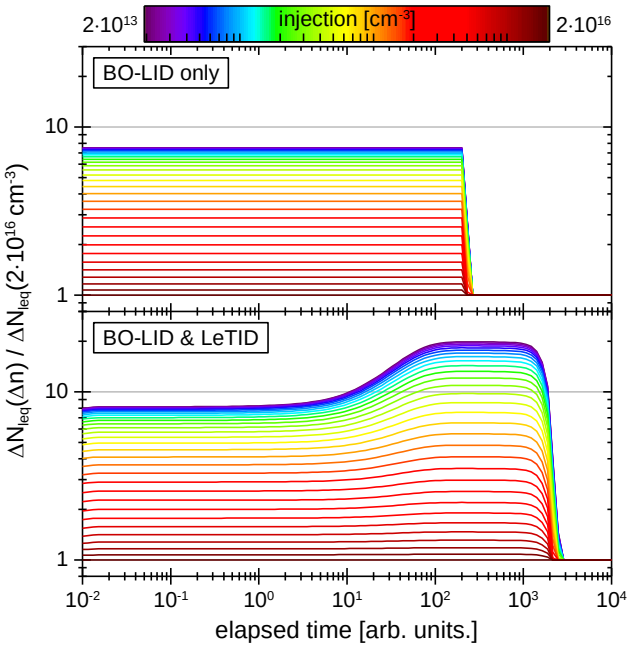

Fig. 6. Time-resolved evolution of the ΔN_{leq} ratio relative to ΔN_{leq} at $\Delta n_{max} = 2{\cdot}10^{16}\,cm^{-3}$ at various color-coded injection levels Δn in *scenarios A & B*. ($T = 300\,K$, $p_0 = 1{\cdot}10^{16}\,cm^{-3}$)

However, already a closer look at $\tau_{eff}(t)$ reveals a peculiar feature hardly compatible with single defect dynamics (see Fig. 4): the exact position of minimum lifetime shifts to longer times the lower the injection is. This feature can be seen even more clearly in total ΔN_{leq} where the red curves (higher injection) already drop after $t = 10^1$, but the blue/violet curves (lower injection) remain constant or even increase, and it can be highlighted even more by plotting not only ΔN_{leq} but rather the ratio of ΔN_{leq} at different injection levels. This is exemplarily shown in Fig. 6 for both, *scenario A & B* with respect to $\Delta n_{max} = 2{\cdot}10^{16}\,cm^{-3}$ (being the highest available injection level). While the ratio remains perfectly constant over time for all injection levels in *scenario A* (Fig. 6 top), it changes characteristically in *scenario B* (Fig. 6 bottom) after $t = 10^1$ as LeTID gradually becomes the dominant lifetime limiting factor. Eventually, the ratio stabilizes on a higher level being characteristic for LeTID when regeneration of BO-LID is almost complete. The higher ΔN_{leq} ratio level is a consequence of the higher assumed τ_p/τ_n ratio of LeTID ($\tau_p/\tau_n = 30$) compared to BOLID ($\tau_p/\tau_n = 10$). The abrupt drop in Fig. 6 in long-term is an artifact due to limited calculation accuracy as infinitesimal small numbers are divided up there.

C. Scenario C: BO-LID, LeTID & FeB dissociation in parallel

Unfortunately, iron is a common contaminant in silicon with an enormous impact on lifetime in p-type silicon even in small concentrations as can be seen in Fig. 2. And even more unfortunate, FeB pairs present after dark storage react to light- and temperature treatments typically used in light-induced degradation studies by dissolving/releasing Fe_i and thus the

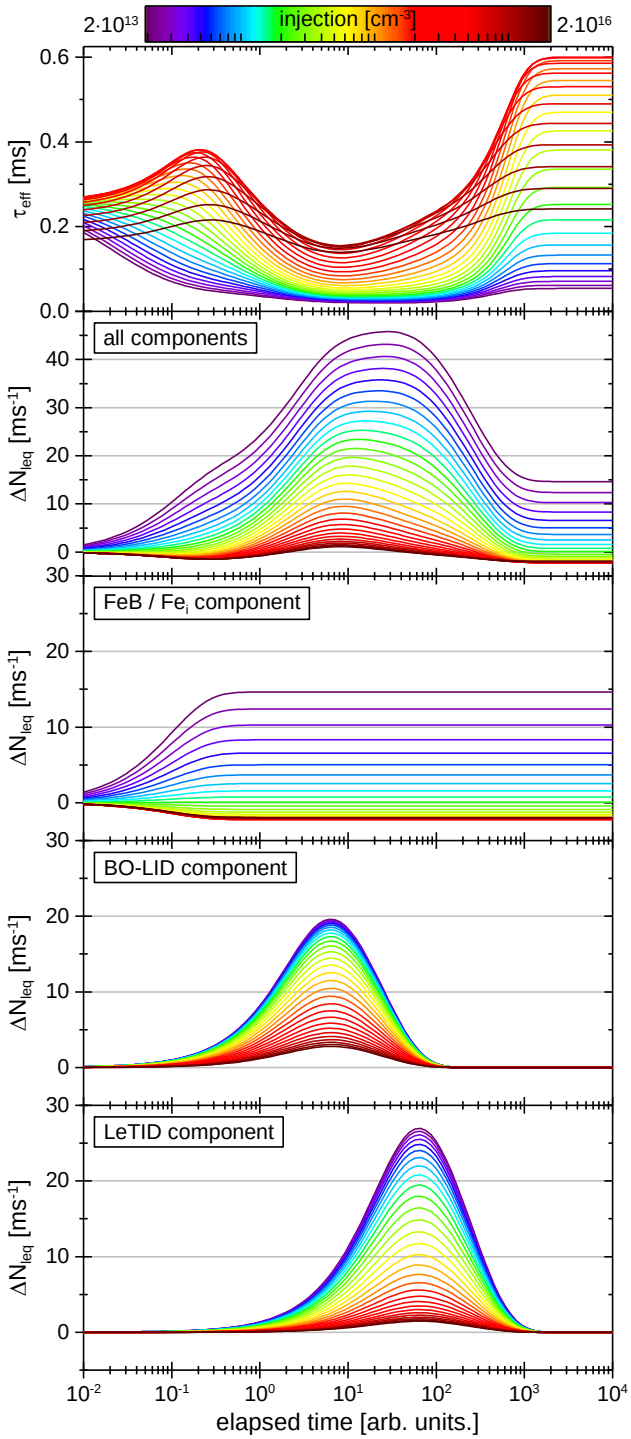

Fig. 7. Time-resolved evolution of the effective lifetime τ_{eff} and derived lifetime-equivalent defect density ΔN_{leq} (in total and for FeB/Fe_i, BO-LID and LeTID seperately) at various color-coded injection levels Δn in *scenario C*. ($T = 300\,K$, $p_0 = 1{\cdot}10^{16}\,cm^{-3}$)

changing influence of iron does not cancel out when ΔN_{leq} is calculated. FeB dissociation is accounted for in *scenario C* assuming initial FeB and Fe_i concentrations of $5{\cdot}10^{10}\,cm^{-3}$ and $0\,cm^{-3}$, respectively, and a decay constant of 0.1.

Figure 7 shows the simulation results of *scenario C*. As discussed in the context of Fig. 3, the dissociation of FeB pairs results in positive ΔN_{leq} values below the cross-over point ($\Delta n_{cop} \sim 2{\cdot}10^{14}\,cm^{-3}$) and negative ΔN_{leq} values above the cross-over point. In consequence, total ΔN_{leq} is reduced at high injection levels (orange/red) and even turns temporarily and in long-term negative. In contrast, total ΔN_{leq} is permanently increased for low injection levels (violet/blue). Even though the ΔN_{leq} component of both, BO-LID and LeTID, vanishes in long-term, total ΔN_{leq} does not except for $\Delta n_{cop} \sim 2{\cdot}10^{14}\,cm^{-3}$ (green) where the ΔN_{leq} component vanishes anyway. Hence one could conclude that regeneration of either BO-LID or LeTID is incomplete if ΔN_{leq} is evaluated at injection levels above the cross-over point or seems to be "more than complete" at injection levels above the cross-over-point. As the latter is maybe counter-intuitive, one could conclude as well that the sample was initially already degraded to some extent.

The iron dynamics related change of sign hampers the injection-dependent analysis analogous to Fig. 6 as well. Hence, it is highly advisable to suppress the influence of iron in light-induced degradation experiments as much as possible, *e.g.*, by using optimized gettering processes. Alternatively, preparing the FeB/Fe_i subsystem to a well-defined state, *e.g.*, by either completely associating the FeB pairs (by sufficiently long dark storage at low temperature) or dissociating the FeB pairs (by intense illumination) for each lifetime measurement. If this is not possible, analyzing defect dynamics at an injection level close to the cross-over point at least minimizes the influence of iron.

VI. Examples for Misinterpretation

As discussed before, it is important to note that the lifetime-equivalent defect density ΔN_{leq} may strongly depend on injection Δn. Unfortunately, there is plenty of room for misinterpretations if injection dependency is ignored. The following two examples shall demonstrate this. *Scenario D* deals with varying background bulk lifetime in different grains in mc-Si in combination with LeTID. It is noteworthy that laterally inhomogeneous surface passivation quality on Cz-Si and FZ-Si would result in a similar situation. *Scenario E* deals with varying iron contamination in different grains of mc-Si in combination with the dissociation of FeB pairs.

A. Scenario D: LeTID and varying background lifetimes

It is a common feature of mc-Si that contaminants and crystal defects are inhomogeneously distributed and that bulk lifetime varies from grain to grain, especially if a wafer originates from the brick edge. Consider the following situation: A first, "good" grain features an injection-independent background lifetime $\tau_{bg,good}$ of 300 µs. A second, "bad" grain features an injection-independent background lifetime $\tau_{bg,bad}$ of only 33 µs. Again, doping level p_0 is chosen to $1{\cdot}10^{16}\,cm^{-3}$. Effective lifetime τ_{eff}, including surface- and intrinsic-related lifetime components (see Fig. 2), of the two grains is shown in Fig. 8 (solid lines). In both grains, LeTID is assumed to occur with the same (lifetime-equivalent) defect density which corresponds to a fully injection-dependent LeTID-related lifetime component with $\tau_{LeTID} = 100\,\mu s$ at $\Delta n = 1{\cdot}10^{15}\,cm^{-3}$ (red line). Degraded effective lifetime $\tau_{eff,deg}$ including the LeTID-related lifetime component is then given by the dashed lines.

As mc-Si is known to be laterally inhomogeneous, LID studies often rely on (lifetime-calibrated) photoluminescence imaging to quantify changes in local effective lifetime τ_{eff}. In many cases, a constant volume generation rate G (excitation photon flux) is used implying a local (steady-state) injection

$$\Delta n = G \cdot \tau_{eff} \tag{7}$$

In principle, an injection gradient between adjacent regions would provoke a compensation current, but this shall be omitted here for the sake of simplicity. Assuming a constant photon flux equivalent to 1 sun, resulting in a volume generation rate G_0 of $1.25{\cdot}10^{19}\,cm^{-3}s^{-1}$, yields the specific injection levels marked in Fig. 8 that are, of course, the lower, the lower the effective lifetime is.

A calculation of apparent ΔN_{leq} values in each grain according to Eq. 1, completely ignoring that the individual τ_{eff} was determined at different injection levels, yields the marked values in Fig. 8 (bottom) which clearly differ. Thus one would conclude that the bad grain suffers more from LeTID even though the extent of LeTID was chosen similarly in both grains – a clear misinterpretation simply because apparent ΔN_{leq} was not determined at the same injection level.

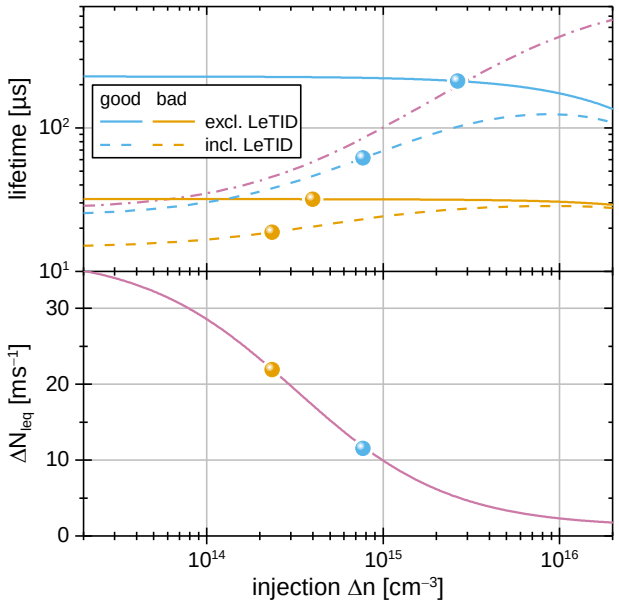

Fig. 8. (top) Injection-dependent effective lifetimes τ_{eff} of the good and bad grain including LeTID (solid lines) and excluding LeTID (dashed lines) as well as the LeTID-related lifetime component (red dash-dotted line). Injection obtained under constant generation conditions is marked for each curve. (bottom) Lifetime-equivalent defect density ΔN_{leq} of LeTID and the apparent ΔN_{leq} in the two grains. (T = 300 K, $p_0 = 1{\cdot}10^{16}\,cm^{-3}$)

B. Scenario E: Inhomogeneous Fe distribution

It is a common feature in mc-Si as well that contaminants, like iron, are inhomogeneously distributed across a wafer [28], [29]. For example, in-diffusion from the crucible walls results in higher contaminant (iron) densities closer to the respective wafer edges. Consider the following scenario: A first, highly (hi) iron-contaminated grain initially features after dark storage $[FeB]_{hi} = 5{\cdot}10^{11}\,cm^{-3}$. A second, lowly (lo) iron-contaminated grain features $[FeB]_{lo} = 1{\cdot}10^{11}\,cm^{-3}$. Apart from Fe_i or FeB, only surface and intrinsic recombination (see Fig. 2) shall limit effective lifetime of the boron-doped p-type material ($p_0 = 1{\cdot}10^{16}\,cm^{-3}$). The effective lifetime curves in the two grains with iron being associated with or dissociated from boron are shown in Fig. 9. However, for the sake of discussion, the experimenter shall be unaware of this iron contamination while he applies illumination within a LID experiment starting after dark storage. Thus iron is in the FeB state during the first measurement and in the Fe_i state for later measurements.

As it was done in *scenario D*, local effective lifetimes τ_{eff} are determined with a constant volume generation rate G. Figure 9 exemplarily illustrates the respective τ_{eff} for $G = ⅓{\cdot}G_0$ as well. Again, ignoring that τ_{eff} was determined at different injection levels, apparent ΔN_{leq} due to the unexpected dissociation of FeB pairs is calculated for both grains in dependence of volume generation rate G. Figure 10 depicts the relation of apparent ΔN_{leq} and generation for both grains and especially for the highlighted generation $G = ⅓{\cdot}G_0$. As can be seen, apparent ΔN_{leq} strongly depends on the choice of generation and on the iron contamination level. For $G = ⅓{\cdot}G_0$ (⅓ sun) it looks, at first glance, as if local defect density has increased in the highly iron-contaminated grain due to applied illuminated annealing whereas it seems to have decreased in the lowly iron-contaminated grain. However, evaluation at $G = 1{\cdot}G_0$ (1 sun) yields a different result: here it appears that local defect density has decreased in both grains.

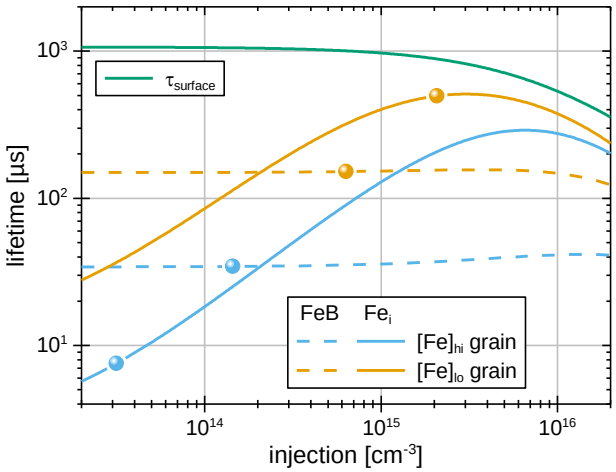

Fig. 9. Injection-dependent effective lifetimes τ_{eff} of the highly and lowly iron-contaminated grain in the associated (dashed lines) and dissociated FeB state (solid lines). The points mark the injection obtained with a generation rate of $⅓{\cdot}G_0$. ($T = 300\,K$, $p_0 = 1{\cdot}10^{16}\,cm^{-3}$)

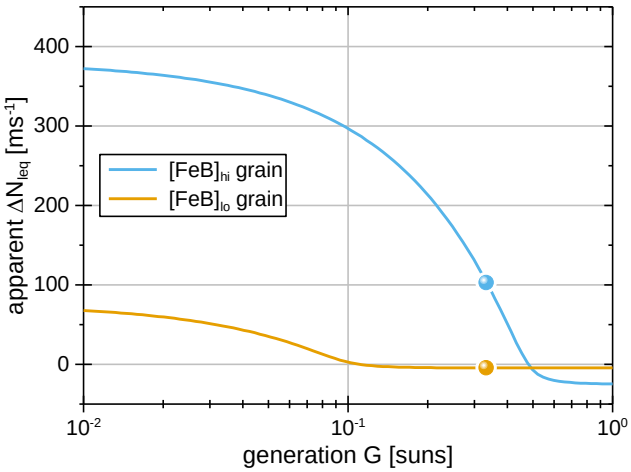

Fig. 10. Apparent lifetime-equivalent defect density ΔN_{leq} in the highly and lowly iron-contaminated grain in dependence of normalized volume generation rate G. ($T = 300\,K$, $p_0 = 1{\cdot}10^{16}\,cm^{-3}$)

Again, the reason for this misinterpretation is due to ignoring injection dependence in combination with being unaware that the sample is iron-contaminated.

As long as obtained injection for a certain generation rate remains above the cross-over point of the FeB/Fe_i system, the ΔN_{leq} ratio corresponds to the assumed initial $[FeB]_{hi}$ / $[FeB]_{lo}$ ratio of 5 in between the two grains even though apparent ΔN_{leq} is negative. However, if injection drops below the cross-over point, which is easier to achieve for low τ_{eff} due to high iron density, ΔN_{leq} turns positive and then gradually increases with decreasing generation.

As can be seen from Fig. 10, there is a certain window in between $½{\cdot}G_0$ and $⅒{\cdot}G_0$, where injection is already below the cross-over-point ($\Delta n_{cop} \sim 2{\cdot}10^{14}\,cm^{-3}$) in the highly iron-contaminated grain but still above it in the lowly iron-contaminated grain. The highlighted points for $G = ⅓{\cdot}G_0$ in Figs. 9 and 10 illustrate this situation.

V. Conclusion

The lifetime-equivalent defect density ΔN_{leq}, being a direct measure of changes in actual defect density in systems comprising only one changing defect species, can be a valuable approach for the quantification of defect dynamics.

However, in situations where more than one defect species is involved, total ΔN_{leq} corresponds to the inseparable sum of individual ΔN_{leq} components. But even then, the characteristic injection dependence of the individual ΔN_{leq} components can be exploted to separate the individual defect species in light-induced degradation experiments, at least when the individual defect species exhibit differing kinetics.

In contrast, ignoring the specific injection dependence of ΔN_{leq} can lead to serious misinterpretations as demonstrated in examples on LeTID and FeB dissociation.

ACKNOWLEDGEMENTS

Part of this work was supported by the German Federal Ministry for Economic Affairs and Energy under contract numbers 0324080C, 0325877C and 0324204B. The content is the responsibility of the author.

REFERENCES

[1] S.W. Glunz, S. Rein, W. Warta, J. Knobloch, and W. Wettling, "Degradation of carrier lifetime in Cz silicon solar cells," Sol. Energ. Mat. Sol. Cells, vol. 65, pp. 219–229, 2001.

[2] K. Bothe and J. Schmidt, "Electronically activated boron-oxygen-related recombination centers in crystalline silicon," J. Appl. Phys., vol. 99, 013701, 2006.

[3] B. Lim, F. Rougieux, D. Macdonald, K. Bothe, and Jan Schmidt, "Generation and annihilation of boron–oxygen-related recombination centers in compensated p- and n-type silicon," J. Appl. Phys., vol. 108, 103722, 2010.

[4] P. Hamer, B. Hallam, M. Abbott, C. Chan, N. Nampalli, and S. Wenham, "Investigations on accelerated processes for the boron-oxygen defect in p-type Czochralski silicon," Sol. Energ. Mat. Sol. Cells, vol. 145, p. 440, 2016.

[5] J. Lindroos and H. Savin, "Review of light-induced degradation in crystalline silicon solar cells," Sol. Energ. Mat. Sol. Cells, vol. 147, pp. 115–126, 2016.

[6] T. Niewelt, J. Schön, W. Warta, S.W. Glunz, and M. C. Schubert, "Degradation of crystalline silicon due to boron–oxygen defects," IEEE J. Photovolt., vol. 7(1), pp. 383–398, 2017.

[7] D. Bredemeier, D. Walter, and J. Schmidt, "Light-induced lifetime degradation in high-performance multicrystalline silicon: Detailed kinetics of the defect activation," Sol. En. Mat. Sol. Cells, vol. 173, pp. 2–5, 2017.

[8] D. Chen, M. Kim, B.V. Stefani, B.J. Hallam, M.D. Abbott, C.E. Chan, R. Chen, D.N.R. Payne. N. Nampalli, A. Ciesla, T.H. Fung, K. Kim, and S.R. Wenham, "Evidence of an identical firing-activated carrier-induced defect in monocrystalline and multicrystalline silicon," Sol. Energ. Mat. Sol. Cells, vol. 172, pp. 293–300, 2017.

[9] T. Niewelt, F. Schindler, W. Kwapil, R. Eberle, J. Schön, and M.C. Schubert, "Understanding the light-induced degradation at elevated temperatures: Similarities between multicrystalline and floatzone p-type silicon," Prog. Photovolt. Res. Appl., vol. 26, pp. 533–542, 2018.

[10] M.A. Jensen, A. Zuschlag, S. Wieghold, D. Skorka, A.E. Morishige, G. Hahn, and T. Buonassisi, "Evaluating root cause: The distinct roles of hydrogen and firing in activating light- and elevated temperature-induced degradation," J. Appl. Phys., vol. 124, 085701, 2018.

[11] D. Sperber, A. Schwarz, A. Herguth, and G. Hahn, "Bulk and surface-related degradation in lifetime samples made of Czochralski silicon passivated by plasma-enhanced chemical vapor deposited layer stacks," Phys. Status Solidi A, vol. 215, 1800741, 2018.

[12] D. Sperber, A. Herguth, and G. Hahn, "On improved passivation stability on highly-doped crystalline silicon and the long-term stability of regenerated Cz-Si," Sol. Energ. Mat. Sol. Cells, vol. 185, pp. 277–282, 2018.

[13] W. Shockley and W.T. Read, "Statistics of the recombinations of holes and electrons," Phys. Rev., vol. 87, pp. 835–842, 1952.

[14] R.N. Hall, "Electron-hole recombination in germanium," Phys. Rev., vol. 87, p. 387, 1952.

[15] A. Herguth, "On the lifetime-equivalent defect density: Properties, application and pitfalls," IEEE J. Photovolt, *in press, DOI: 10.1109/JPHOTOV.2019.2922470*

[16] K. Ramspeck, S. Zimmermann, H. Nagel, A. Metz, Y. Gassenbauer, B. Birkmann, and A. Seidl, "Light induced degradation of rear passivated mc-Si solar cells," Proc. 27th Eur. Photovolt. Sol. Energy Conf., Frankfurt/Main, Germany, 2012, pp. 861–865.

[17] F. Fertig, K. Krauß, and S. Rein, "Light‐induced degradation of PECVD aluminium oxide passivated silicon solar cells," Phys. Status Solidi RRL, vol. 9, pp. 41–46, 2015.

[18] F. Kersten, P. Engelhart, H. C. Ploigt, A. Stekolnikov, T. Lindner, F. Stenzel, and J. W. Müller, "Degradation of multicrystalline silicon solar cells and modules after illumination at elevated temperature," Sol. Energ. Mat. Sol. Cells, 142, pp. 83–86, 2015.

[19] A.E. Morishige, M.A. Jensen, D.B. Needleman, K. Nakayashiki, J. Hofstetter, T.A. Li, and T. Buonassisi, "Lifetime spectroscopy investigation of light-induced degradation in p-type multicrystalline silicon PERC," IEEE J. Photovolt., vol. 6(6), pp. 1466–1472, 2016.

[20] G. Zoth and W. Bergholz, "A fast, preparation-free method to detect iron in silicon," J. Appl. Phys., vol. 67, pp. 6764–6771, 1990.

[21] L.J. Geerligs and D. Macdonald, "Dynamics of light-induced FeB pair dissociation in crystalline silicon," Appl. Phys. Lett., vol. 85, pp. 5227–5229, 2004.

[22] D. H. Macdonald, L. J. Geerligs, and A. Azzizi, "Iron detection in crystalline silicon by carrier lifetime measurements for arbitrary injection and doping," J. Appl. Phys., vol. 95, pp. 1021-1028, 2004.

[23] L.J. Geerligs, G. Coletti, and D. Macdonald, "On accurate and quantitative measurements of iron-concentration in multicrystalline silicon by iron-boron pair dissociation," Proc. 21st Eur. Photovolt. Sol. En. Conf., Dresden, Germany, 2006, pp. 692–695.

[24] K.R. McIntosh and L.E. Black, "On effective surface recombination parameters," J. Appl. Phys., vol. 116, 014503, 2014.

[25] A. Herguth and G. Hahn, "Kinetics of the boron-oxygen related defect in theory and experiment," J. Appl. Phys., vol. 108, 114509, 2010.

[26] A. Herguth and B. Hallam, "A generalized model for boron-oxygen related light-induced degradation in crystalline silicon," AIP Conf. Proc., vol. 1999, 130006, 2018.

[27] A. Herguth, "On the meaning(fullness) of the intensity unit 'suns' in light induced degradation experiments," Energ. Proc., vol. 124, pp. 53–59, 2017.

[28] D. Macdonald, J. Tan and T. Trupke, "Imaging interstitial iron concentrations in boron-doped crystalline silicon using photoluminescence," J. Appl. Phys., vol. 103, 073710, 2008.

[29] A.Y. Liu, Y.C. Fan and D. Macdonald, "Interstitial iron concentrations across multicrystalline silicon wafers via photoluminescence imaging," Prog. Photovolt. Res. Appl., vol. 19, pp. 649–657, 2011.